Intercalation of Inorganic Fullerene-like Structures Yields Photosensitive Films and New Tips for Scanning Probe Microscopy

M. Homyonfer,[†] B. Alperson,[†] Y. Rosenberg,[‡] L. Sapir,[§] S. R. Cohen,[⊥] G. Hodes,[†] and R. Tenne*,[†]

Contribution from the Department of Materials and Interfaces, Department of Physical Services, and Department of Chemical Services, Weizmann Institute, Rehovot 76100, Israel, and Center for Materials Research, Tel-Aviv University, Ramat Aviv 69978, Israel

Received October 15, 1996[⊗]

Abstract: Evaporation of metals, like W, Mo, V, and In, in the presence of water vapor and subsequent sulfidization has yielded bulk quantities of nested fullerenes, nanotubes, and structures with negative curvature (inorganic fullerene-like−IF). Dissolving alkali-metal salts into the water source afforded alkali-metal intercalation and staging ($n = 6$) of the IF structures after sulfidization. The intercalated moieties were found to be stable in air and even in water. The intercalated IF structures could be dispersed in alcoholic suspensions, and electrophoretic deposition from the suspensions yielded thin films of the IF particles. The films of intercalated IF showed respectable and time-invariant photoeffects. Furthermore, low adhesion and robust tips for scanning probe microscopy were prepared by depositing intercalated IF film on Si tips. Other applications, which are currently investigated, are briefly mentioned.

Introduction

Nanoclusters of various inorganic layered compounds, like metal dichalcogenides−MX_2 (M = Mo, W; X = S, Se), are known to be unstable in the planar form and to form a hollow cage−inorganic fullerene-like (IF-MX_2) structures like nested fullerenes and nanotubes.[1−3] Not surprisingly, nanoparticles of hexagonal boronitrides with graphite-like structures behaved similarly.[4,5] Furthermore, nested fullerene-like polyhedra of MoS_2 were synthesized at room temperature by a stimulus from an electron beam[6] in analogy to carbon nested fullerenes[7] and also by application of an electric pulse from the tip of a scanning tunneling microscope (STM).[8]

Intercalation of carbon nanotubes with alkali metal atoms from the vapor phase was recently described.[9] The intercalated films were found to arrange in a stage−1 ($n = 1$) superlattice, i.e., alkali-metal layers were stacked between each two carbon layers. The composite nanostructures were found to disintegrate when exposed to air, and complete shattering of the nanotubes (exfoliation) was obtained upon immersion in water. The intercalation of 2H-MoS_2, 2H-WS_2, and other metal dichalcogenide compounds was discussed in detail,[10−12] but staging was not observed in either of the former compounds, i.e., the alkali atoms were found to have a random distribution. Here too, deintercalation occurs upon exposure to air and exfoliation upon immersion in water.

In the present work, a new method is described for the synthesis of large quantities of IF structures. This method affords also intercalation of the IF structures with various metal atoms, which has a remarkable influence on the solubility of these structures in aprotic solvents. The formation of stable suspensions from the intercalated IF materials permits deposition of thin films, with a range of potential applications. Of these, the use of such films as the photosensitive element in solar cells and for the fabrication of inert STM tips is described in the present work.

Experimental Section

Scheme 1 illustrates a flow chart of the processes used for synthesizing alkali-metal intercalated IF structures and for fabricating the films, from, e.g., intercalated IF-WS_2. The first step in this hierarchy consists of synthesizing oxide powder in a modified vacuum deposition apparatus (see Figure 1a). For that purpose, a W (or other metal) wire was heated and evaporated in the presence of water vapor. Metal or metal oxides could be evaporated from tungsten boats, but this would usually lead to mixed tungsten-metal oxide (and sulfide after sulfidization) nanoparticles. To intercalate the IF particles with metal atoms, metal-doped oxide nanoparticles were first prepared. This was done by dissolving 10^{-3}−10^{-2} M of alkali-metal salts, like NaCl, etc., in the water and coevaporating it together with the heated wire to form alkali-doped metal oxides. Further experimental details of the apparatus and the work protocol are described in the legend to Figure 1. As a result of this process, a blue metal oxide film accrued on the walls of the bell-jar. In the second step of Scheme 1, the oxide powder was

* Author to whom correspondence should be addressed.
† Department of Materials and Interfaces, Weizmann Institute.
‡ Tel-Aviv University.
§ Department of Physical Services, Weizmann Institute.
⊥ Department of Chemical Services, Weizmann Institute.
⊗ Abstract published in *Advance ACS Abstracts,* March 1, 1997.

(1) Tenne, R.; Margulis, L.; Genut, M.; Hodes, G. *Nature* **1992**, *360*, 444.
(2) Feldman, Y.; Wasserman, E.; Srolovitz, D. J.; Tenne, R. *Science* **1995**, *267*, 222.
(3) Feldman, Y.; Frey, G. L.; Homyonfer, M.; Lyakhovitskaya, V.; Margulis, L.; Cohen, H.; Hodes, G.; Hutchison J. L.; Tenne, R. *J. Am. Chem. Soc*. **1996**, *118*, 5362.
(4) Stephan, O.; Ajayan, P. M.; Colliex, C.; Redlich, Ph.; Lambert, J. M.; Bernier P.; Lefin, P. *Science* **1994**, *266*, 1683.
(5) Chopra, N. G.; Luyken, R. J.; Cherrey, K.; Crespi, V. H.; Cohen, M. L.; Louie, S. G.; Zettl, A. *Science* **1995**, *269*, 966.
(6) José-Yacamán, M.; Lopez, H.; Santiago, P.; Galván, D. H.; Garzón I. L.; Reyes, A. *Appl. Phys. Lett.* **1996**, *69*, 1065.
(7) Ugarte, D. *Nature* **1992**, *359*, 707.
(8) Homyonfer, M; Mastai, Y; Hershfinkel, M; Volterra, V; Hutchison, J. L; and Tenne, R *J. Am. Chem. Soc*. **1996**, *118*, 7804.
(9) Zhou, O.; Fleming, R. M.; Murphy, D. W.; Chen, C. H.; Haddon, R. C.; Ramirez A. P.; Glarum, S. H. *Science* **1994**, *263*, 1744.
(10) Brec, R.; Rouxel, J. *Intercalation in Layered Materials* Dresselhaus, M. S., Ed.; NATO ASI Series B: Physics, Plenum Press: New York, 1986; Vol. 148, pp 75−91.
(11) Friend, R. H; Yoffe, A. D. *Adv. Phys*. **1987**, *36*, 1.
(12) Somoano, R. B.; Hadek, V.; Rembaum, A. *J. Chem. Phys.* **1973**, *58*, 697.

S0002-7863(96)03585-8 CCC: $14.00

Scheme 1. Flow Chart I llustrating the Various Steps in the Fabrication of the Photosensitive IF-WS_2 (MoS_2) Films[a]

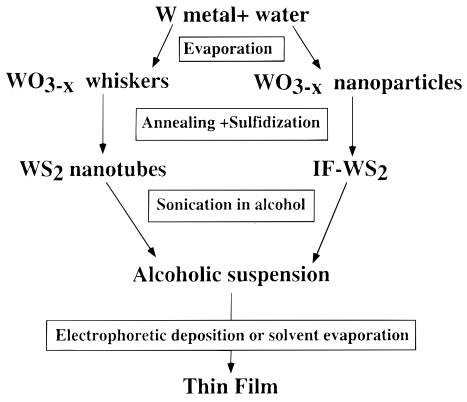

[a] To obtain the suspensions, a 50 mg portion of IF particles (nanotubes) was mixed with 50 mL of ethanol, and the mixture was sonicated for 5 min.

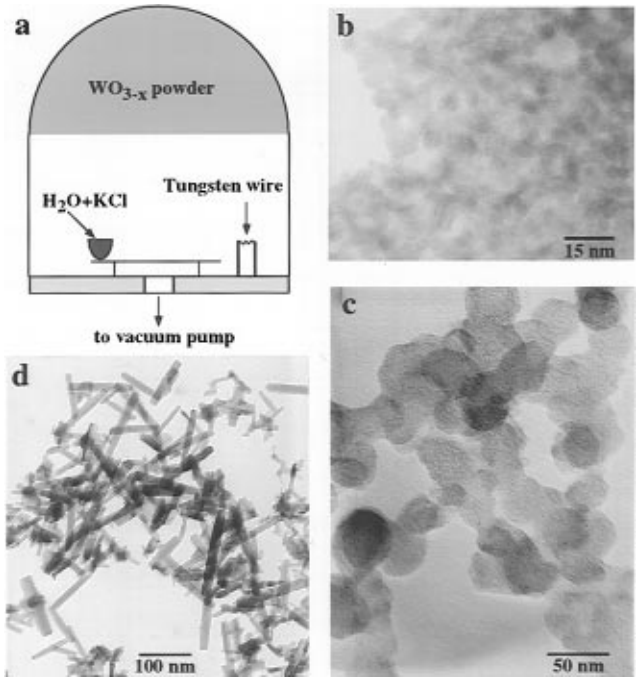

Figure 1. (a) Schematic representation of the evaporation apparatus used for the synthesis of the oxide nanoparticles and whiskers. In the first stage, the bell-jar was evacuated to ca. 10^{-5} Torr. The tungsten (molybdenum) wire was cleaned by heating it close to its melting temperature for a few minutes, after which the system was allowed to cool to ambient temperatures. The bell-jar was opened, and a beaker with about 3 mL of water was inserted. Upon evacuation to about 10^{-3} Torr, the water in the beaker froze. At this point, the gate valve was closed and the W wire heated again. After a few minutes, the wall of the bell-jar was covered with a blue oxide powder which was collected for characterization and further processing. The size of the oxide particles and their shape could be varied according to the process parameters, such as pumping speed, vacuum, etc. TEM images of the oxide precursors: (b) small (<10 nm) and (c) large (ca. 50 nm) spherical particles; (d) whiskers.

converted into a sulfide with nested fullerene or nanotube structures (generically known as inorganic fullerene-like material-IF), by annealing the oxide in a reducing atmosphere with H_2S gas.[3]

Stable alcoholic suspensions of the IF particles were obtained by mixing a few milligrams of the intercalated IF powder in 3 mL of ethyl alcohol and sonification of the mixture (third step in Scheme 1). The solubility of the IF particles was found to be proportional to the amount of intercalant, whereas IF particles containing >8% of alkali-metal atoms were totally stable, and nonintercalated IF particles did not form stable suspensions at all.

Next, deposition of intercalated IF films from the suspensions was accomplished (fourth step in Scheme 1), using two alternative routes: solvent evaporation or electrophoretic deposition onto gold substrates, which were prepared according to a published procedure.[13] In general, electrophoretic deposition resulted in more adhesive films and was therefore preferred in the present study.

Transmission electron microscopy (TEM) was used for lattice imaging and electron diffraction of the nanoparticles. The composition of the oxide and sulfide nanoparticles was established using energy-dispersive X-ray analysis (EDS Link model ISIS) mounted on a high resolution TEM (200 kV, JEOL Model 2010) with probe size of 5 nm. The alkali metal concentration in the oxide precursor was determined by inductive coupled plasma (Spectro- Spectroflame ICP) analysis and by X-ray photoelectron spectroscopy (Kratos Axis-HS using monochromatized Al Kα radiation). X-ray powder diffraction (Scintag Theta-Theta XRD equipped with liquid nitrogen cooled Ge solid state detector, and Cu Kα anode) was used to determine the crystallinity and phase of the oxide (sulfide).

Scanning force microscope (SFM) and scanning tunneling microscope (STM) were used to image the IF film surface both in noncontact and contact modes (SFM) and in photoassisted imaging mode (STM). All SPM work was done on a Topometrix TMX 2010 Discoverer system. For contact mode force microscopy, the probes were either Si_3N_4 (Park Scientific) or single crystal Si (Nanoprobe) microfabricated tips. IF tips were prepared by electrophoretic deposition on the latter, as described below. For intermittent contact mode, Si probes (Nanoprobe) with resonance frequency of 260−320 kHz were used. STM was performed using mechanically cut PtIr tips. For the photoassisted measurements, a 650 nm laser diode (Toshiba) was focused to the junction so that the focused fluence was 30−50 mW/cm^2. The laser was operated either CW or modulated at 3−5 kHz. In the latter case, the modulated current signal was processed by a lock-in amplifier (SRS530).

Photocurrent measurements and electrolyte electrotransmission (EET) were carried out on a standard computerized photoresponse set-up, equipped with a light source, monochromator, potentiostat, lock-in amplifier, voltage modulator, and optics. For these measurements, a copper wire was attached to the gold substrate of the IF film, and the entire electrode, except for the front surface, was covered with an insulating resin. A standard photoelectrochemical cell with Pt mesh as counter electrode and Pt wire as a reference electrode was used.

Results

Using the evaporation method described above, the particle sizes (7−50 nm) and shapes could be varied by changing the experimental conditions. Figure 1b,c shows TEM images of the oxide nanoparticles. Their composition was found from XPS to vary between $WO_{2.9}$ and $WO_{2.5}$. Tungsten oxide is known to have stable unstoichiometric phases with O/W ratio varying in this range[14] (*vide infra*). The alkali metal content varied between 4 and 8 atomic %. An XRD study indicated that the oxide precursor was mainly amorphous. Using a lower vacuum (10^{-3} Torr) and higher pumping speed, which produced more water vapor, a blue powder consisting mainly of oxide whiskers with an average size of 300 nm was deposited on the bell-jar (Figure 1d).[15] Careful control of the evaporation conditions was imperative for maintaining a high yield of the oxide nanoparticles and whiskers. In particular, the metal cleaning process prior to the evaporation was found to be very important for the success of the process.

(13) a. Golan Y., Margulis L.; Rubinstein I. *Surf. Sci.* **1992**, *264*, 312; b. Alperson, B.; Cohen, S.; Rubinstein, I.; Hodes, G. *Phys. Rev. B* **1995**, *52*, R17017.

(14) Wells, A. F. *Structural Inorganic Chemistry*, 3rd ed., Oxford University Press: Oxford, 1962; p 468.

(15) For the preparation of still longer oxide whiskers (average length 500 nm), the water vapor was saturated with a mixture of transition metal salts (1:1): $CoCl_2 \cdot 6H_2O/FeCl_3$ and $NiCl_2/CoCl_2 \cdot 6H_2O$ (20% v/v). However, no direct evidence for the intercalation of the transition metal atoms into the IF paritcles has been obtained so far.

The sulfidization process of oxide nanoparticles and the production of IF materials of various kinds have been described.[2,3] The sulfidization starts at the outermost surface of the oxide, and the oxide core is progressively consumed and converted into sulfide. For the IF-WS_2 material, a solid−gas reaction between WO_3 and H_2S has been adopted, while gas phase reaction between MoO_3 and H_2S was undertaken for the synthesis of IF-MoS_2.[16] Interestingly, the alkali-metal doped molybdenum-oxide powder obtained in the present synthetic apparatus is much less volatile than the nonintercalated nanoparticles studied before. Therefore, the simpler solid−gas reaction between MoO_3 powder and H_2S gas was adopted for the synthesis of IF-MoS_2 in the present study. It was found that during the early stages of the sulfidization process, reduction and crystallization of the oxide core takes place. In particular, $W_{18}O_{49}$ was observed as a stable intermediate phase in the sulfidization of (nonintercalated) oxide nanoparticles.[3] It is likely that this or a similar suboxide phase is also formed during the present sulfidization process. A detailed investigation of the phase transformation of the oxide core using high resolution TEM is currently underway.

Following the sulfidization of the oxide nanoparticles, IF structures with a near to spherical shape or polyhedral topology were obtained from the quasi-spherical oxide particles (Figure 2a), while nanotubes, which were closed at both ends, were obtained from the oxide whiskers (Figure 2b). The size of the IF particles retained the size of the oxide precursor particles. An abundance of T-bars, closed from three ends, and in one case even a torus (Figure 2c) structure, all showing negative curvature,[17−19] were obtained by a similar procedure. The number of closed sulfide layers in the IF structures could be controlled through the firing time. Because the reaction can be interrupted at any time, macroscopic amounts of fullerene-like structures and nanotubes with different numbers of sulfide layers and an oxide core including single, double, or multiple layers (with oxide core) or fully converted (hollow) IF could be synthesized.

In general, the intercalation process is not limited to the metallic atoms, and intercalation of solvent molecules from solutions cannot be avoided.[20] However, in the present process, water molecules, if at all incorporated into the oxide particles, would be outgassed during the sulfide synthesis. Indeed, no evidence for the intercalation of solvent molecules into the host lattice was found. Furthermore, since no prismatic edge planes $(11\bar{2}0)$ exist in these closed structures, intercalation of solvent molecules, which makes the 2H platelets susceptible to solvent intercalation and exfoliation,[20,21] was avoided.

The above method is rather versatile and is not limited to IF of Mo or W chalcogenides. Figure 3 presents the lattice image of VS_2 fullerene-like particles which were obtained with the same apparatus. IF structures of γ-In_2S_3 were also obtained but are not shown. The starting material for IF-VS_2 was V_2O_5 which was heated in a molybdenum boat in the presence of water vapor. This explains the observation that some of the nanoparticles were mixed IF-$V_xMo_{1-x}S_2$. It is likely that Na intercalation facilitates the synthesis of IF-VS_2, since it has been established previously that Na intercalation promotes 2H-VS_2 formation.[11] The precursor for In_2O_3 was In shot heated in a Mo boat. This shows the versatility of the present procedure, which in fact can be used for the synthesis of IF structures from virtually any metal-chalcogenide having a layered-type structure.

The IF powder synthesized in the second step formed very stable suspensions in various alcohols upon sonication (third step of Scheme 1). IF-MS_2 powders, which were synthesized

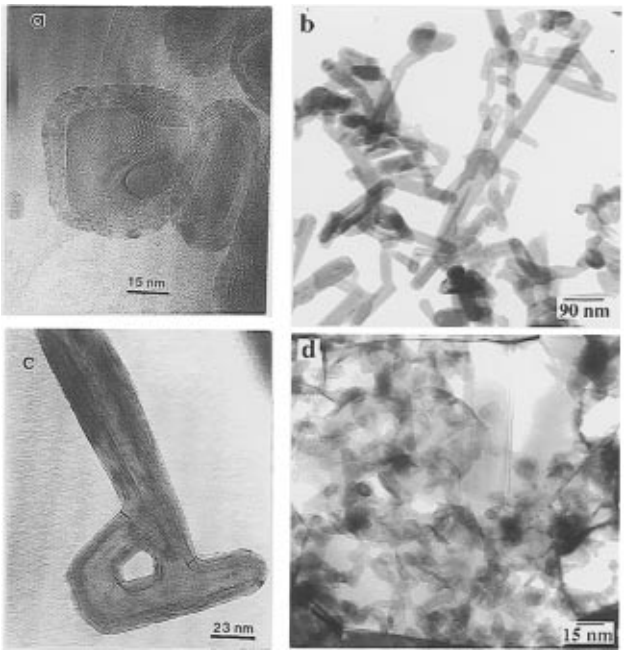

Figure 2. TEM images of tungsten-sulfide nanoparticles obtained from the oxide precursors shown in Figure 1: (a) oblate and quasi-spherical IF particles; (b) nanotubes; and (c) torus exhibiting negative curvature (Schwartzite). Figure 2d shows a full-fledged IF-WS_2 film on a Au substrate. The IF film was deposited by first evaporating a gold film (35 nm) on mica and annealing it to 250 °C for 12 h, which resulted in {111} textured Au crystallites with a typical size of 1 mm.[14] The IF films were obtained by applying a bias of 20 V between the gold cathode and a Pt foil which were immersed in the (intercalated) IF suspension. IF films up to 500 nm in thickness were obtained by this procedure.

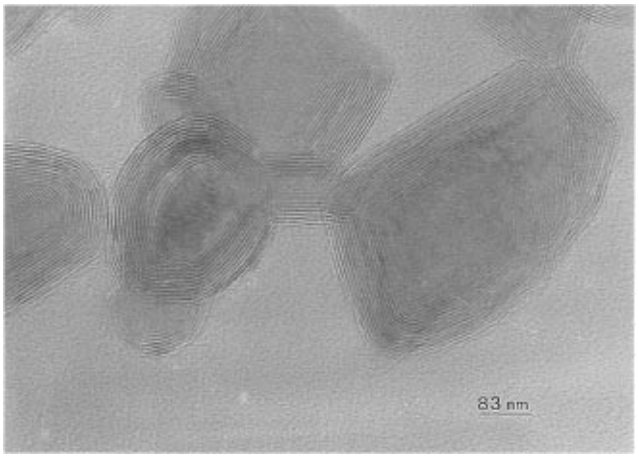

Figure 3. TEM micrograph showing the lattice image of VS_2 nested fullerene-like particles obtained from the respective oxide nanoparticles which were produced by the apparatus of Figure 1a. Lattice spacing (c) is 0.61 nm.

(16) For the production of IF-WS_2 from tungsten-oxide nanoparticles, the oxide powder was spread very loosely on the surface of the quartz reactor. The sulfidization of the first top few oxide layers must take place before coalescence of the oxide particles occurs, otherwise platelets of 2H-WS_2 would form. In the case of the volatile molybdenum oxide, the preliminary sulfidization occurs in the gas phase before the nanoparticles settle on the quartz susceptor. The subsequent conversion of the oxide core into sulfide takes place on the susceptor, and coalescence of the nanoparticles is avoided altogether.

(17) Iijima, S.; Ichihashi T.; Ando,Y. *Nature* **1992**, *356*, 776.
(18) Terrones, H.; Terrones M.; Hsu, W. K. *Chem. Soc. Rev.* **1995**, 341.
(19) Dunlap, B. *Phys. Rev. B.* **1992**, *46*, 1933.
(20) Somoano R. B.; Woollam, J. A., *Intercalated Layered Materials*; Lévy, F., Ed.; D. Reidel Publishing Company: Dordrecht, 1979; pp 307−319.
(21) Jonson, P.; Frindt, R. F.; Morrison, S. R. *Mater. Res. Bull.* **1986**, *21*, 457.

according to previously reported procedures,[2,3] did not form stable suspensions even after prolonged sonication. These results indicate that the intercalation of alkali metal atoms in the van der Waals gap of the IF particles led to a partial charge transfer to the host lattice which increased the polarizability of the nanostructures, enabling them to disperse in polar solvents. The transparency of the suspensions and their stability increased with the amount of alkali-metal intercalated into the IF structures. Suspensions prepared from IF powder (both fullerene-like particles and nanotubes) which contained large amount of intercalant (>5%) was found to be virtually indefinitely stable. The optical absorption of the IF suspensions was very similar to that of thin films of the same nanoparticles. Details of the optical properties of IF films is deferred to a forthcoming publication.[22]

In the next step, IF films were deposited on a gold substrate by electophoretic deposition. Given the chemical affinity of sulfur to gold, it is not surprising that electrophoretic deposition led to relatively well-adhering IF films. Furthermore, some selectivity with respect to the IF sizes and number of MS_2 layers in the films was achieved by varying the potential of the electrode. The thickness of the film was controlled by varying the electrophoresis time. Figure 2d presents a TEM image of a very thin film (tens of nm) of IF particles together with the gold substrate. Since the nonintercalated IF particles do not form stable suspensions, films of such material were obtained by electrophoresis from vigorously sonicated dispersions of the IF powder. Alternatively, IF films were prepared by evaporating the solvent from a dip-coated metal substrate; this method, however, resulted in poorly-adhering films.

Using XPS analysis, the alkali content of the IF particles was found to vary from 4−10 atom %, depending on the parameters of preparation of the oxide precursor and the subsequent sulfidization process. X-ray diffraction patterns of IF-WS_2 and 2H-WS_2 powders were measured using CuKα radiation (Figure 4). The most pronounced evidence for the formation of fullerene-like particles is the shift of the (0002) Bragg diffraction peak toward lower angles and the simultaneous broadening of this peak. The shift reflects the strain relief mechanism associated with folding of S-W-S layers.[2,3] The peak broadening is due to the reduced domain size for coherent X-ray scattering in the direction perpendicular to the basal (000l) plane. The expansion along the *c*-axis of the IF particles (ca. 2−4%) may also reflect the random distribution of the intercalated atoms, at least in a subgroup of the IF particles. However, the variation between the lattice spacing (d_{0002}) of the IF particles, which are doped with different alkali atoms, is small (6.35 Å for Na compared to 6.45 Å for K). The appearance of superstructure Bragg diffraction peaks at small angles (Figure 4) strongly indicates the presence of an ordered IF phase with staging.[9,23] The three (000l) Bragg reflections allude to a sixth stage (n = 6) in IF-WS_2. The repeat distance between the adjacent intercalated layers varies from 36.7 Å for Na to 38.9 Å with K.[24] These results suggest that two populations of fullerene-like particles exist, one having ordered dopant atoms (staging) with n = 6, the other with randomly distributed alkali atoms. Since the number of MS_2 layers in the IF particles varies from about four to ten, those particles with fewer than six layers cannot exhibit staging, and consequently a random distribution of the alkali metal atoms is thermodynamically favored in this case. It was reported[12] that intercalation of alkali metal atoms into the lattice of 2H-MoS_2 did not lead to staging, and, furthermore, the intercalated material was found to be extremely sensitive to air and moisture. Finally, two additional weak diffraction peaks with lattice spacing of 2.81 and 3.03 Å were observed. These peaks were assigned to a microphase of $NaNO_3$, which might be formed through the reaction of forming gas (N_2-95%/H_2-5%) with oxygen during sulfidization of the oxides.

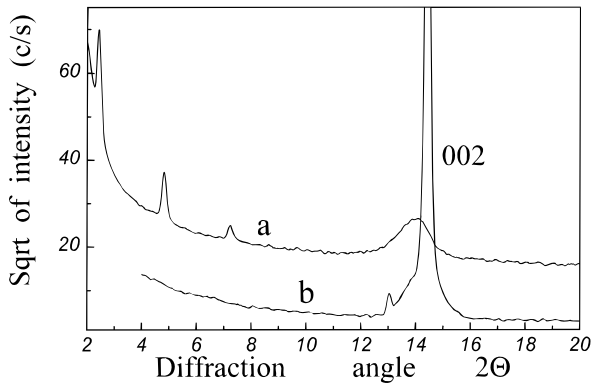

Figure 4. (a) Powder diffraction of IF-WS_2 with sodium as intercalant and (b) WS_2 platelets (the peak at 13° is assigned to the CuK_β). To preclude parasitic scattering, the specimens were deposited on background-free single crystal quartz plates. Step size was 0.005°, and exposure time was 6 s/point. The square root intensity presentation was used to increase the dynamic range of the figure.

The optical absorption spectra of intercalated 2H-MoS_2 did not show appreciable changes for alkali metal concentrations less than 30%, where a transition into a metallic phase at room temperature and a further transition into a superconductor at about 3−7 K were reported.[10,20] Since the concentration of the intercalating metal atoms did not exceed 10% here, no changes in the optical transmission spectra were anticipated nor were found to occur. The intercalation of alkali atoms in the IF particles also induces n-type conductivity of the host.

The prevalence of dangling bonds on the prismatic faces of 2H-WS_2 crystallites leads to rapid recombination of photoexcited carriers. Consequently, the performance of thin film photovoltaic devices of layered compounds has been disappointing. The absence of dangling bonds in IF material suggested to us that this problem could be alleviated here. Therefore the photocurrent response of IF-WS_2 films in selenosulfate solutions was examined and compared to that of 2H-WS_2 films. The response was found to be very sensitive to the density of dislocations in the film. Curve **a** of Figure 5 shows the quantum efficiency (number of collected charges/number of incident photons) of a typical nested fullerene-like (WS_2) film with a low density of dislocations, as a function of the excitation wavelength. On the other hand, films having nested fullerene-like particles with substantial amounts of dislocations exhibited a poor photoresponse and substantial losses at short wavelengths (curve **b**), which indicate that the dislocations impair the lifetime of excited carriers in the film.[25] Films of nanotubes also showed substantial photoresponse (curve **c**). Finally, films made of 2H-WS_2 platelets (each about 1 μm in size), which are known to have many recombination centers on the prismatic edges (1120), did not exhibit any measurable photoresponse under comparable conditions. The photocurrent decreased with negative bias, reaching zero at −1.0 V vs the Pt foil counterelectrode, thus affirming that the intercalated IF particles were n-type. The photoresponse of the IF films did not show any degradation

(22) Frey, G. L. et al., to be published.

(23) Dresselhaus M. S.; Dresselhaus, G. *Adv. Phys.* **1981**, *30*, 139.

(24) Attempts to identify the superlattice of the intercalated atoms by electron diffraction was unsuccessful so far. It is likely that the low concentration of the alkali-metal atoms, and the large repeat unit distance, which entails diffraction spots near the central bright ring of the electron microscope beam prevents such measurements.

(25) Lewerenz, H. J.; Heller, A.; DiSalvo, F. *J. Am. Chem. Soc.* **1980**, *102*, 1877.

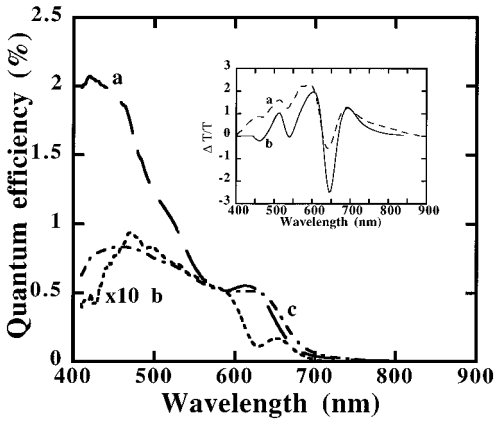

Figure 5. Photoresponse spectra of thin films of IF-WS_2: (a) IF film with low density of dislocations; (b) film consisting of IF particles with a high density of dislocations; and (c) nanotubes. The inset presents EET spectra of (a) dislocation-free IF film and (b) nanotubes. The EET spectra were obtained by measuring the transmission spectrum while superimposing an ac modulation of 0.45 V on the photoelectrode.

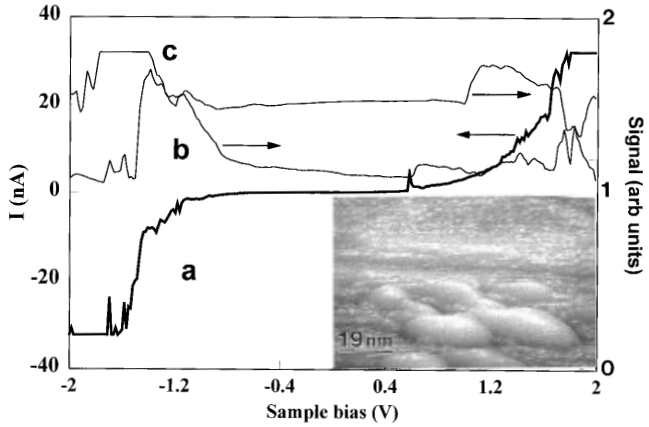

Figure 6. Scanning tunneling current spectroscopy of fullerene-like WS_2 films deposited on a gold substrate, using a Pt-Ir tip. Curve **a** is an I-V plot in the dark showing a bandgap of about 1.6 eV; curve **b** shows background ac signal without illumination; and curve **c**- shows an I-V plot under modulated 650 nm illumination, attenuated by a factor of 4. The modulation signal represents the lock-in output in arbitrary units, whereas the I-V signal is in nA. See text for further description. The peaks at negative sample bias in curves **b** and **c** are an artifact due to capacitive pickup. Prior to the measurements, the sample was wetted with selenosulfate solution and then dried for about 30 min. Inset: topography taken with a sample bias of 50 mV; a current setpoint of 0.7 nA, under cw laser illumination, showing a group of fullerene-like structures on a gold terrace. This illumination induces strong tunneling current over the IF, allowing it to be seen as protrusions on the surface (contrast to curve **a**).

after 48 h of continuous illumination. Electrolyte electrotransmission (EET) spectra of the IF films were also recorded.[26] The inset of Figure 5 shows such a spectrum, which clearly reveals the direct excitonic transitions of the film at 2.02 (A exciton) and 2.4 eV (B exciton), respectively.

STM was used to probe the photoresponse of individual IF particles electrodeposited on a gold film. Initially, STM measurements were made in the dark. Both I/V spectroscopy and topographic images were made. The I/V spectroscopy yielded either ohmic behavior (not shown) corresponding to exposed gold regions on the surface or a currentless region centered around 0 V bias corresponding to the "bandgap" of the individual IF particle (Figure 6a). These data must be interpreted in the framework of a metal−semiconductor−metal structure. The log of the current increases linearly with voltage, behavior which is associated with Poole conduction.[27] The slight current enhancement in the positive sample bias region is expected for the n-type IF under study. The I/V curve could be used to determine tunneling conditions which do not sweep the IF particles away by the tip: the bias was set to 1.5 V with current setpoint < 1 nA. Photoresponse was then measured by illuminating the junction with modulated 650 nm light. The laser was applied after observing no photo effect when using 0.5 W, mildly focused white light. We do not expect thermal effects such as tip expansion to be present under our working conditions of relatively low-power laser light.[28] Using the lock-in output as a measure of the photoresponse, two effects can be observed by comparing Figures 6b,c. First, the signal level is raised over the entire voltage scan. Secondly, significant enhancement of the signal was observed at positive sample bias. Note that curve c on Figure 6 was attenuated by a factor of 4 to keep it on scale. The peak at negative bias seen in both curves is an artifact due to capacitative pickup.

The current enhancement under illumination was exploited to improve the STM imaging of the individual IF particles. Using a bias voltage of 50 mV, conditions which would not allow observation of the IF in the dark, the sample was imaged under CW illumination. The resulting image is shown in the inset. The contrast between the IF particles and the gold substrate stems from the photosensitivity of the former, which produced large current contrast even under small bias. This effect also indicates that the response is due to photocurrent, not photovoltage which would have a much smaller current dependence on distance. Choice of small bias sets the tip-surface distance and hence impedance to a relatively low value, which increases sensitivity to the photocurrent. The photoassisted STM imaging was obtained only after the film was wetted by a drop of a selenosulfate solution. Recently, a few authors discussed the influence of electrolyte solutions in mediating the charge transfer in films consisting of semiconducting nanoparticles (e.g., refs 29 and 30).

We must also consider the effect of the tip proximity in the STM experiments: tip-induced band-bending due to a surface space-charge region can lead to a reduced current for the lower bias values. Although the Na concentration is high enough to lead to a very small space-charge region if there was full charge transfer from the alkali metal atoms to the host, the actual charge transfer is only partial. This may explain the difference between measured bandgap (1.6 eV) and published values (1.3 eV).[31] Coulomb charging cannot be a significant factor in determining the bandgap as this effect would only increase the measured bandgap by a few meV for our 30 nm radius IF particles. The asymmetry observed in curve **c** of Figure 6, is due to the n-type nature which led to the assymetry in curve **a** of Figure 6 as discussed above. Here, the illumination aids to flatten the bands and enhance the effect.

The photocurrent observed in the IF film can be explained by separation of photogenerated charges by a space charge layer in the semiconductor, which however is not likely to be very large in these nanostructures. A second possible explanation may be that the photocurrent flow is determined by preferential

(26) Bordas, J. *Optical and Electrical Properties*, in the series *Physics and Chemistry of Materials with Layered Structures*; Lee, P. A., Ed.; D. Reidel Publishing Company: Dordrecht, 1976; pp 145−230.

(27) Geddes, N. J.; Sambles, J. R.; Parker, W. G.; Couch, N. R.; Jarvis, D. J.; *J. Phys. D: Appl. Phys.* **1990**, *23*, 95.

(28) Hamers, R. J.; Merkert, K. *Phys. Rev. Lett.*. **1990**, *64*, 1051.

(29) Gerischer, H.; Heller, A. *J. Phys. Chem.* **1991**, *95*, 5261.

(30) Hodes, G.; Howell I. D.; Peter, L. M. *J. Electrochem. Soc.* **1992**, *139*, 3136.

(31) Kam, K. K.; Parkinson, B. A. *J. Phys. Chem.* **1982**, *86*, 433.

trapping/transfer of either photogenerated electrons or holes. In this scenario, the free charge defines the position of the Fermi level upon illumination. There are a number of possible explanations for the modest quantum efficiencies exhibited by the illuminated films: potential barrier between the nanoparticles or between the nanoparticles and the back contact impede the flow of the carriers from the front surface into the back contact; insufficient doping of the IF film leads to internal resistance within the nanoparticles; surface trapping of carriers by imperfections and dislocations, etc. Photosensitive films of this kind can be used for various purposes, including the photoremediation of water, photochemical storage of solar energy, etc. The d−d nature of the photoexcitation process prohibits degradation of the film photoresponse over extended periods of time.[32]

We found that the relatively low affinity of the IF to any surface made their imaging with scanning force microscopy (SFM), problematic. Using contact-mode SFM with a Si or Si_3N_4 cantilever/tip, the fullerene-like particles were brushed aside, and the images were blurry and irreproducible. This was true both at ambient and low humidity conditions and using cantilevers with lateral (torsional) spring constants of 3−250 N/m, with the lowest workable loading force, typically 5−20 nN. Using the noncontact mode, the IF were clearly seen, which proves that this imaging problem is related to the affinity between the tip and surface. To reduce the interaction between the tip and the IF, a thin layer of IF-WS_2 particles was deposited from the alcoholic suspension, using the Si cantilever/tip as a cathode. Formation of geometrically and chemically well-defined tips is of great interest to the SFM community. Prior to this work, Ducker et al.[33] successfully attached micron size colloidal spheres to the cantilever of an SFM tip and measured force laws in electrolyte solution. A geometrically well-defined tip with radius 2 orders of magnitude smaller allow us to investigate a completely different range of forces. Dai et al. have recently reported attachment of carbon nanotubules to the apex of an SFM tip.[34] With this new tip, clear images of the IF film surface were obtained in contact mode (Figure 7). This "IF-tip" was used to image several surfaces without degradation, before eventually falling off. We have yet to determine the reason for the stability of this composite Si/IF tip compared to evaporated or electrodeposited IF film. Presumably, the stability of this composite tip is related to the presence of a high electric field because of the sharp tip, which makes a more stable bond between the IF particle and the Si tip. By imaging a Nb thin film surface with sharp features (General Microdevices), we estimate this tip radius to be 20 nm, which coincides with a typically-sized IF particle. This new composite tip is now being considered for SFM-imaging of various objects.

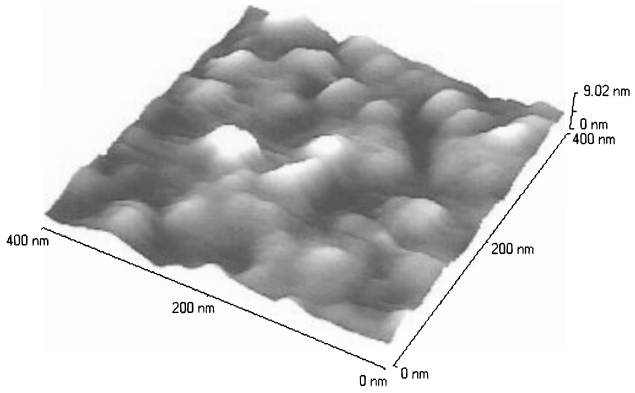

Figure 7. Contact-mode SFM image of the IF-WS_2 film used in the experiments of Figures 4, obtained with the Si/IF composite tip, which was prepared by electrophoretic deposition of IF film on the Si tip. To prepare the IF coated tip, the Si cantilever was inserted into the IF-suspension with an average particle size of 30 nm. A Pt foil served as anode, and a bias of 20 V was applied between the cathode and anode for ca. 1 min.

In a series of new experiments, the IF suspension is mixed with precursors to form a sol-gel film. The resulting translucent glass exhibits the typical absorption spectra of IF.[35] This development opens the way for a host of new applications of IF in optics and electro-optics.

Acknowledgment. We are grateful to Dr. H. Cohen and Prof. M. Talianker for the assistance with the XPS and EDS measurements, respectively. This project was supported by grants from the Minerva Foundation, Munich, Germany, U.S.−Israel Binational Science Foundation, NEDO (Japan), Israeli Ministry of Science and Technology, and the Israeli Ministry of Energy and Infrastructure.

JA963585Z

(32) Tributsch, H. *Struct. Bonding* **1982**, *49*, 127.

(33) Ducker, S. A.; Senden, T. J.; Pashley, R. M. *Nature* **1992,** *353*, 239.

(34) Dai, H.; Hafner, J. H.; Rinzler, A. G.; Colbert, D. T.; Smalley, R. E. *Nature* **1996**, *384*, 147.

(35) Reisfeld R. et al., to be published.